EUROPEAN ORGANIZATION FOR NUCLEAR RESEARCH
ORGANISATION EUROPEENNE POUR LA RECHERCHE NUCLEAIRE

CERN - PS DIVISION

PS/RF/ Note 2002-156
SL-Note-2002-030 (AP)

BENCH MEASUREMENTS OF THE LHC INJECTION KICKER LOW FREQUENCY IMPEDANCE PROPERTIES

F. Caspers, A. Mostacci

Abstract

The LHC injection kicker contains a ceramic tube with inside printed metallic strips as a RF bypass in order to minimise the beam coupling impedance. These strips are capacitively coupled at one side to avoid eddy current during kicker transients. Experimentally it was found already earlier, using bench techniques, that in the region between 10 and 30 MHz certain resonances and thus peaks in the coupling impedance occur, related to the transition of the image current from the “cold conductor" to the bypass strips. The presence of these resonances has been reconfirmed as well as their properties. A practical method for reducing their influence by attaching lossy ferrite rings to the ends of the ceramic pipe is proposed and has partly been tested. As the present measurements were done on a mock-up for this RF bypass, which has limited validity towards higher frequencies, a full scale test should be repeated, once the first prototype of the 3 meter long ceramic chamber with printed bypass strips is available.

Geneva, Switzerland
August 2002

1 Introduction

The present note is intended to document the results of a series of measurements done in August 2002 on the LHC injection kicker. At this time a true prototype of the 3 meter long ceramic tube with shielding strips was not yet available. Thus measurements were done on a mock-up with the real kicker i.e. simulating these strips on the inner surface of the ceramic tube by inserting an isolating (plastic type) foil with similar metallisation. Due to lack of time and manpower, proper RF contacts at the ends could not be implemented since the main objective of the present measurement was to gain better understanding of low frequency resonances around 10-30 MHz. In parallel cross-check tests were done on an electrically much better defined 1 meter long model and both results are compared and discussed. The objective is to point out measurement difficulties at this stage as well as finding a sound strategy to eliminate these resonances by reasonable means (ferrite torus) the low frequency.

2 Measurements on the kicker

The aim of the present measurements was the investigation and possible cure of low frequency resonance of the longitudinal impedance of the LHC dump kicker equipped with a ceramic tube, that is coated inside with printed shielding strips. Such resonances have been already found in earlier measurements [2]. They are considered to be related to the transition of the image current from the "cold conductor" acting as a bypass to the shielding strips. In order to avoid significant perturbation (eddy currents) of the magnetic field during any transients of the kicker, these shielding strips are capacitively coupled to ground and directly coupled at the opposite side. The measurement procedure is defined as follows:

- Insert a wire into the kicker with adequate matching resistors on either side after having checked its characteristic impedance and compared with theory.
- Correct for the matching resistor losses as well as for the mechanical length (artificial reference).
- Try to find practical (compatible with all constrains) means to dampen the resonances.
- Compare the results with results obtained from a simplified 1 meter long laboratory model (coated ceramic tube with cold conductor bypass).

It is already known a priory that the set-up used for the kicker is not valid beyond about 50-100 MHz due to the "quick and dirty" made transitions and RF-contacts at the ends. However the small model with good RF-contacts can provide more reasonable data on the broadband response.

2.1 Matching resistor

The bench set-up is a coaxial line obtained by inserting a Cu-Be wire in the kicker module (DUT). The transition between such a coaxial line and the cable connecting the Vector Network Analyser (VNA) is not automatically matched. Being D the diameter of the inner ceramic chamber supporting the copper stripes and d the diameter of the Cu-Be wire, the characteristic impedance of the coaxial line is ($D = 37 \pm 1$ mm, $d = 0.5$ mm)

$$Z_c = \frac{Z_0}{2\pi} \ln\left(\frac{D}{d}\right) = 258.2 \pm 1.6\ \Omega, \tag{1}$$

where $Z_0 = 377\ \Omega$ is the vacuum characteristic impedance. Thus Z_c is different from the impedance of the cables connecting the VNA (i.e. $Z_{VNA} = 50\ \Omega$, after calibration) and

"external" reflections at the ports will occur.

The characteristic impedance of the coaxial line can also be measured with the "Time Domain Reflectometry" technique, using the time domain option of the HP8753D network analyser. One measures the signal reflected by the unmatched transmission line with a synthesised (unitary) step excitation, the so called "low frequency step" in the VNA jargon. The calibrated S_{22} for the (unmatched) coaxial line is shown in Fig. 1 (left plot) as a function of the delay along the transmission line; the different "stairs" are the multiple reflections at the opposite ends of the structure. At the moment of our measurements, the copper strips are not printed in the inner part of the ceramic chamber (as foreseen in the kicker design), but they are placed on an insulating foil inserted inside the ceramic pipe. The diameter of such a foil is not perfectly constant, as can be deduced from the non-flatness of the first step (between 0 and 22 nsec), as shown in Fig. 1.

From the amplitude $\Delta\Gamma$ of the reflection coefficient at the "first" reflection, it is possible to get the impedance of the coaxial line Z_c, i.e.

$$Z_c = Z_{VNA}\frac{1+\Delta\Gamma}{1-\Delta\Gamma} = Z_{VNA}\frac{1+0.687}{1-0.687} = 269.5\ \Omega, \tag{2}$$

which is reasonably close to the theoretical value of Eq. (1).

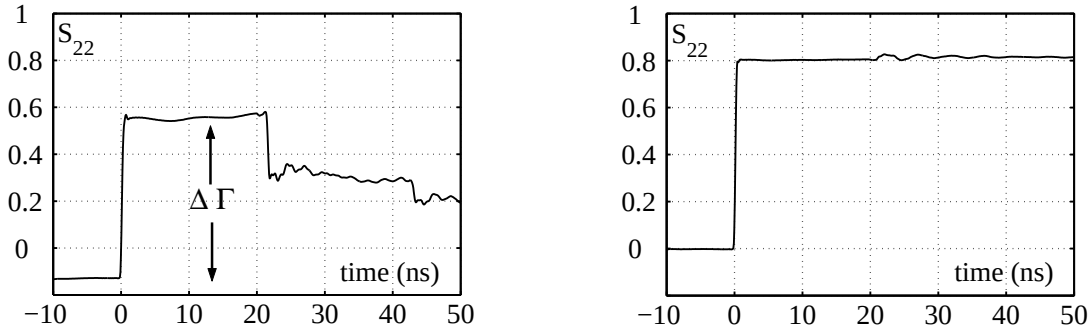

Figure 1: Reflection coefficient measurement analysis in the time domain. The left plot shows multiple reflections in the non-matched coaxial line obtained by inserting a wire (0.5 mm diameter, Cu-Be) along the DUT axis. Adding matching resistors (computed from $\Delta\Gamma = 0.687$), the multiple reflections disappear at the expenses of an increased reflection between DUT and instrument (right plot).

To assure matching for the signals going from the coaxial line (formed by the wire in the DUT) towards the VNA (the so called "internal" matching, [1]), matching resistors can be used (at least in our frequency range). They are soldered at each end of the cable and their value Z_{match} is such that

$$Z_c = Z_{match} + Z_{VNA}.$$

For practical reasons, the two matching resistors actually soldered between the wire and the connectors have nominal value of 200 Ω. The reflection coefficient of the matched line is shown in Fig. 1 (right plot), where the multiple reflections disappeared at the price of an increased reflection of the signal coming from the network (about 80% of the input signal is reflected versus only 69% without resistors on the wire).

2.2 Transmission measurements with the wire

After soldering the matching resistors on each side of the copper wire, we obtain the transmission coefficient S_{21} as depicted in Fig. 2. The upper plot shows its magnitude (in dB) with the low frequency ohmic losses on the matching resistor already subtracted.

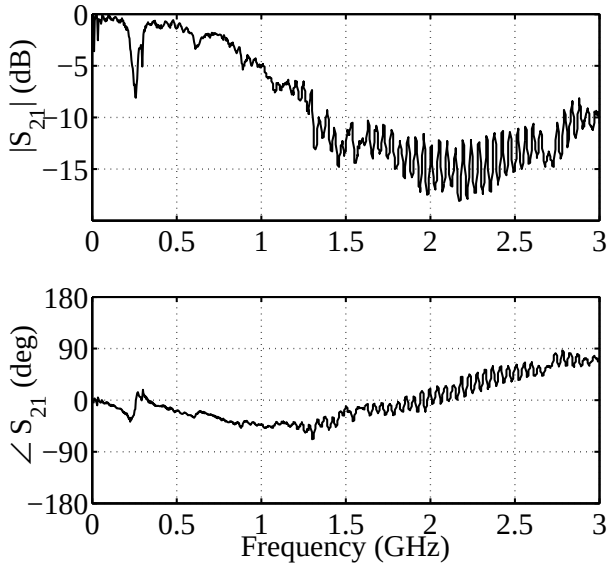

Figure 2: Transmission coefficient (S_{21}) versus frequency for the LHC injection kicker. A Cu-Be wire (0.5 mm diameter) is placed along the DUT axis. Matching resistors (200 Ω) have been mounted at each end of the wire. The amplitude (upper plot) has been corrected from the low frequency losses on the resistors. The lower plot shows the phase of the S_{21} after "time delay connection" (3.23 m). The strong increase if attenuation in S_{21} is due to the poor RF-contacts at each end.

The lower plot shows the phase of S_{21} after the time delay correction according to the (mechanical) length of the line minus the length of the joint used in the calibration (we used the so called "response THRU" calibration [4]). The distance between the two connectors is 3.26 m and the calibration joint is 0.03 m (electrically) long.

To get Fig. 2, the raw data for $|S_{21}|$ are shifted up (so that $|S_{21}| = 0$ at low frequencies) in order to subtract the ohmic losses on the matching resistors. Unfortunately, such losses change with frequency, explaining the fast oscillations in $|S_{21}|$ at frequencies greater than about 1 GHz (the matching resistor impedance changes and the matching condition is not fulfilled anymore).

The frequency behaviour of the two different kinds of matching resistors (deduced from a S_{11} measurement in an individual text box) used in our two set-ups is shown in Fig. 3. The impedance of the one used in the kicker tank is shown in the left plot: it is constant to the nominal value (200 Ω) up to roughly 230 MHz and around 1 GHz its real part is decreased of one half. The fast oscillations visible at high frequencies are due to internal reflections (50 MHz period, 3 m length).

On the contrary, the resistor used in the chamber prototype (sec. 3) has a low frequency value of roughly 235 Ω (the nominal value being 220 Ω), but it already decreases to one half at 550 MHz (Fig. 3, right plot). A small resonance is also clearly visible at 2.1 GHz, but it is due to the connectors used to test the resistors; in fact there is not such effect in the measurement on a reference line using similar resistors, reported in Fig. 6

(left plot).

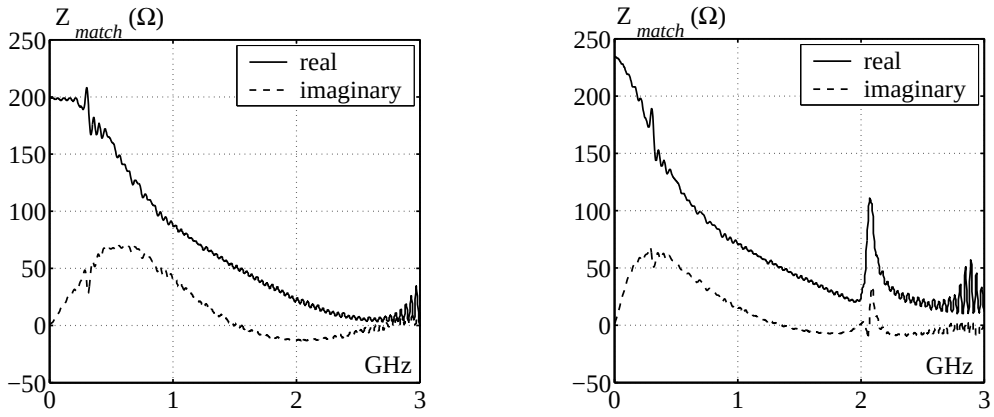

Figure 3: Impedance of the matching resistors versus frequency. The left plot concerns the resistor used in the kicker tank, while the right plot concerns the resistor mounted in the ceramic chamber 1 m long prototype. Fast oscillations beyond 2.5 GHz are due to residual effects from long measurement cables.

The transmission measurement on the kicker tank have been carried out when the copper strips were left floating as well as when they were connected to the kicker tank (as they would be in the final kicker). Figure 4 shows an expanded view from a 0-3 GHz measurement (thus the low number of points), for the "normally" connected strips, i.e. direct contact at one side and capacitively coupled at the other side (dashed line) in comparison to the situation where both sides were directly connected (solid line). The slope in that solid line indicates already , that, due to the poor RF contacts at the end of the kicker tank, these data are not relevant with respect to the coupling impedance beyond 50 or 100 Mhz. In other words: the setup should only be used to investigate the low frequency resonances.

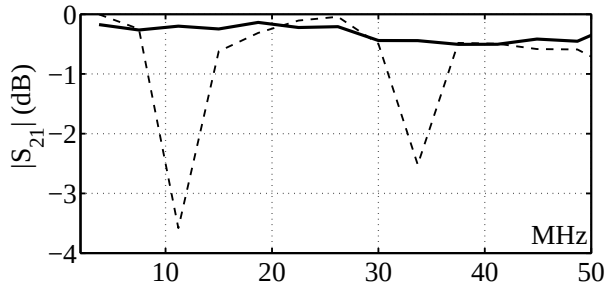

Figure 4: Transmission measurement in the kicker tank. The strips are left first floating (dashed line) and then connected to the tank (solid line). It is an expanded view from a 3 GHz bandwidth trace, thus the number of data point is small.

3 Ceramic chamber with printed metal strips

3.1 Description of the prototype

The ceramic test chamber (with printed strips inside using the same technology as for the final version) as shown in Fig. 5 has good RF-contacts on either side ("**A**" and "**C**" in Fig. 5). One can recognise the two small "SUKO" boxes, containing the matching

resistor as well as the N-connectors at the extremities. The lower part (rectangular steel profile underneath the ceramic tube) serves both as mechanical support and as electrical simulation for the "cold conductor" of the kicker. The "printed" coupling capacitor is visible near the right connector (position "**C**") and has pyramid like "teeth" towards position "**B**". These "teeth" are intended as an RF match (gradual transition for the image current) towards higher frequencies, but maybe finally they will not be mandatory. As the real kicker is seldom available for test we prefer to do as much as possible in this "scale model". However the validity of that model must be proven in particular with respect to the low frequency resonances. As it will be shown in the next sections, these low frequency resonances could also be found for the present model.

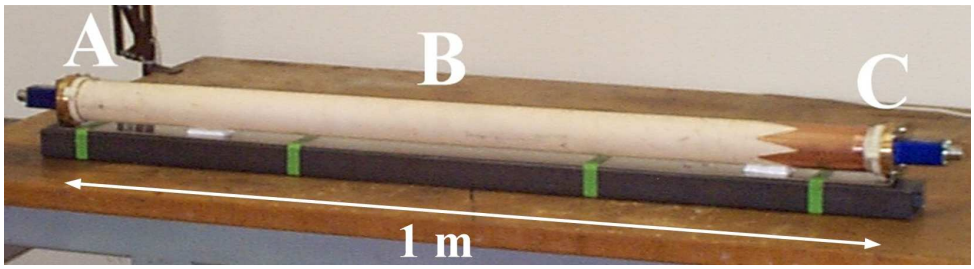

Figure 5: Ceramic chamber with coated copper strips inside.

3.2 Coupling impedance measurement: the method

Following the "coaxial wire technique" [3], a Cu-Be wire is placed on the longitudinal axis of the kicker module (which we call Device Under Test, DUT) and a Vector Network Analyser (VNA) measures the transmission coefficient S_{21} between the two extremities.

The coaxial transmission line formed by kicker module + wire is mismatched with respect to the instrument (VNA, 50 Ω generator and load impedance) and some matching network has to be used (see sec. 2.1). The coupling impedance can be computed from the transmission parameter S_{21} via the "logarithmic formula":

$$Z_{log} = -2Z_c \ln\left(\frac{S_{21}^{DUT}}{S_{21}^{REF}}\right) \tag{3}$$

where Z_c is the characteristic impedance of the coaxial line and S_{21} is the transmission coefficient (measured by the VNA). REF stands for REFerence measurement: it is a measurement with the same bench set-up (in particular the same matching network) where the DUT is substituted by a reference a lossless line of the same length.

3.3 DUT and REF measurements

The result of transmission measurements for the 1 meter long model are shown in Fig. 6. Here we can also clearly see the impact of the degrading RF performance of the matching resistors. Up to about 500 MHz the transmission for the reference line (Fig. 6, left picture) is rather flat and without undulations. Beyond that frequency we recognize a slow increase in transmission as well an an increase of ondulation (due to increasing mismatch as seen from inside the test chamber). However when using the same resistors for both, the reference and DUT measurement, the ratio of both S-parameters leads to a proper final result (Fig. 7 and Fig. 8).

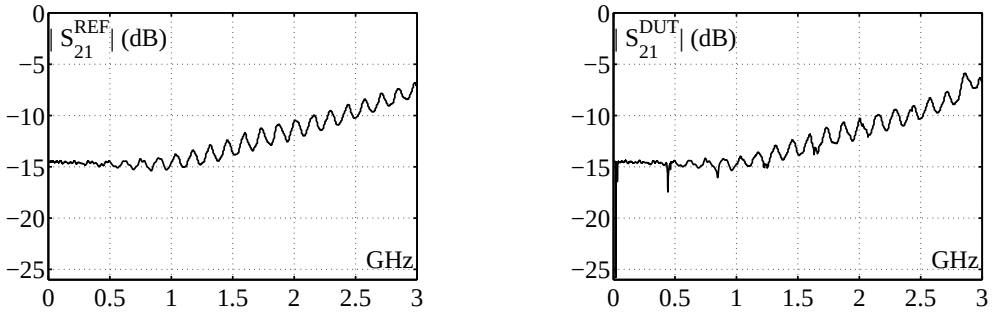

Figure 6: Transmission coefficient for the ceramic chamber with (inside) printed metal strips (S_{21}^{DUT}, right plot) and for a brass pipe of the same dimensions (S_{21}^{REF}, left plot).

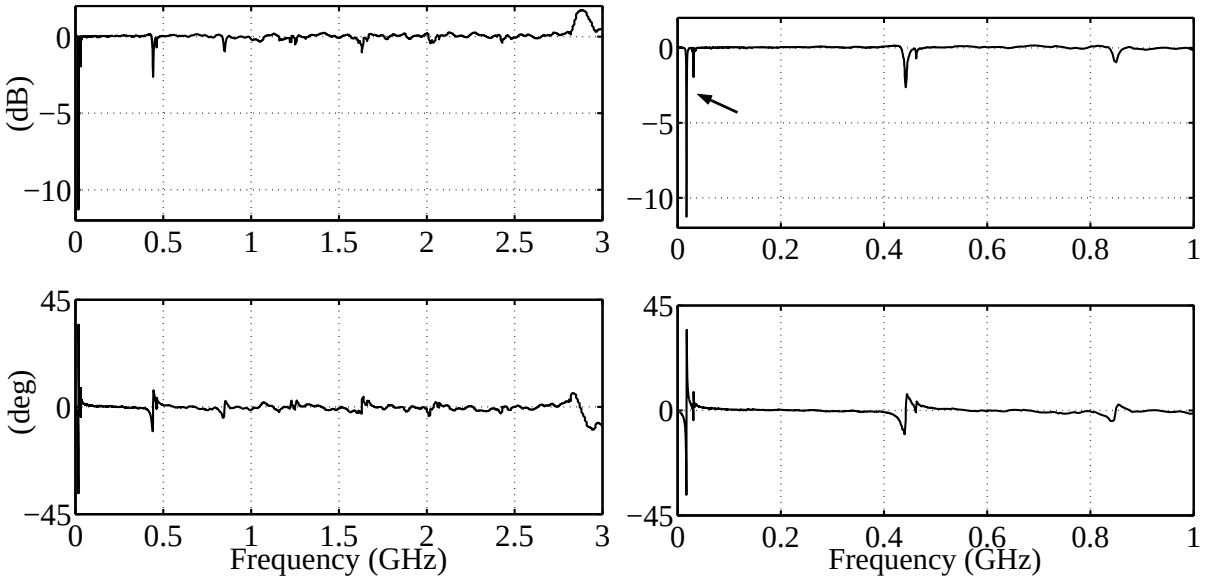

Figure 7: Transmission coefficient ($S_{21}^{DUT}/S_{21}^{REF}$) versus frequency. A Cu-Be wire (0.5 mm diameter) is placed on the ceramic chamber axis. Matching resistors (220 Ω) have been mounted at each end of the wire. The small resonance pointed out by the arrow is due to the not perfectly tightened wire.

3.4 Coupling impedance measurement

Evaluating the S-parameter results for the 1 meter long test model in terms of coupling impedance (Fig. 8) according to the usual procedure (i.e. comparing with a true and not an artificial reference), we can clearly identify several resonances (Fig. 8, left plot) up to 1 GHz. Apart from the already well known low frequency resonance we have seen peaks (e.g. around 0.4 GHz) which were identified as being related to the length of the coupling capacitor.

Part from that the baseline of the impedance is very close to zero (within the noise and drift zone) which shows that the concept of printed strips to be used as RF bypass is healthy. It also shows that the very poor transmission above 1 GHz in Fig. 2 is not relevant for the final version as it either related to the imperfect RF contacts and/or the effect of the copper cladded insulating foil. An interesting finding was the "multiple resonance" around 30 MHz in Fig. 8 (right plot). This is clearly related to an offset wire and did not show up, when the coaxial wire was well centred (as explained in sec. 3.5).

Very likely for the offset case the individual strips of the bypass are excited in an uneven manner and thus start resonating in mutually odd modes finally leading to the 30 MHz resonances shown above.

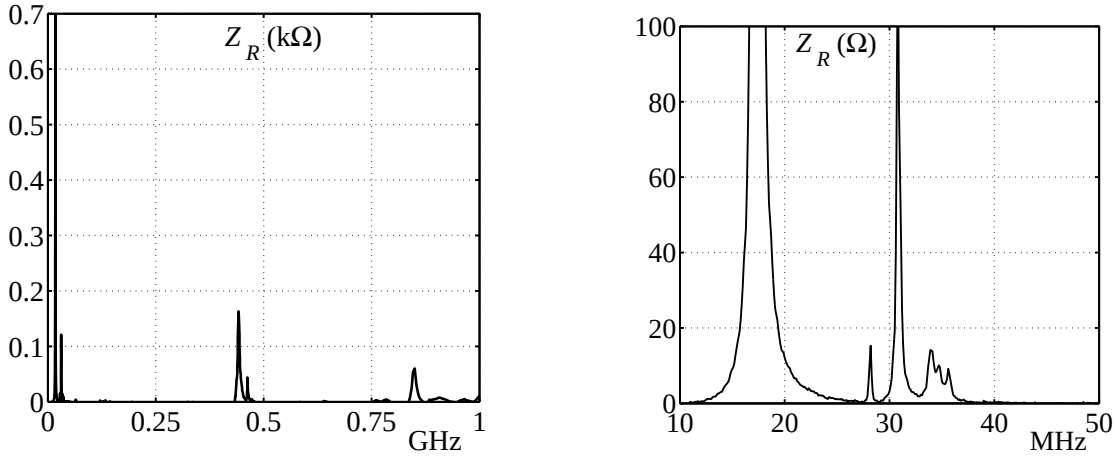

Figure 8: Coupling impedance of the 1 meter long test ceramic chamber with printed metal strips (wire measurement). The right plot is an enlargement at low frequencies of the left plot.

3.5 Effect of the position of the wire

In Fig. 9, we compare the response for a well centred and slightly offset wire. Already a small offset leads to "odd mode" type excitation of the strips and is thus causing additional resonances.

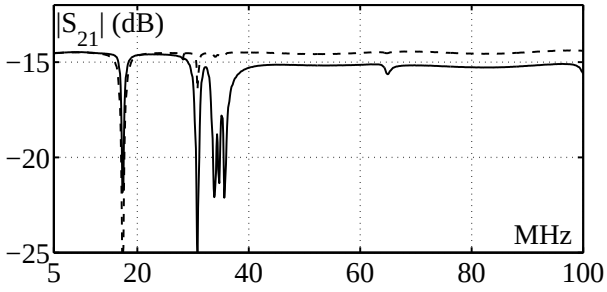

Figure 9: Transmission coefficient $|S_{21}|$ for the ceramic chamber. The solid line is measured when the wire is not perfectly placed along the longitudinal axis (i.e. when the wire is not well tightened). There are additional resonances with respect to the tight wire (dashed line).

3.6 Reducing the resonance peaks

The remaining task is now to find suitable concept to dampen as strongly as possible not only the low frequency resonances around 10-30 MHz but also higher frequency ones. After several test with loading resistors, lossy dielectric material and ferrite blocks, finally ferrite rings were found to be the most efficient and yet applicable material. The successful application of ferrite rings also proves that indeed there are surface current on the outer

surface of the structure. Otherwise we could not get any interaction. Obviously for the real kicker there is the kicker ferrite close to the ceramic shielding pipe and had already (found in earlier measurements) a beneficial effect on that resonance above 200 MHz. However the low frequency problem although reduced (c.f. Fig. 4, compare depth of resonance notch with Fig. 10) still remains and requires further action. The very preliminary positive and promising results when using (simulated i.e. composed by 4 ferrite plates) ferrite rings are shown in Fig. 10. Further work is needed here in particular more detailed tests both on the model and in the real kicker after careful selection of suitable ferrite material (both electrically and for UHV). Another important aspect is a reliable estimate of the losses induced by the beam into these ferrites and potential heating limitations. The ferrite rings (to be installed on either side in the real kicker) could also be used as a torus type transformer with a separate load (heating!) to be attached somewhere else inside the kicker tank.

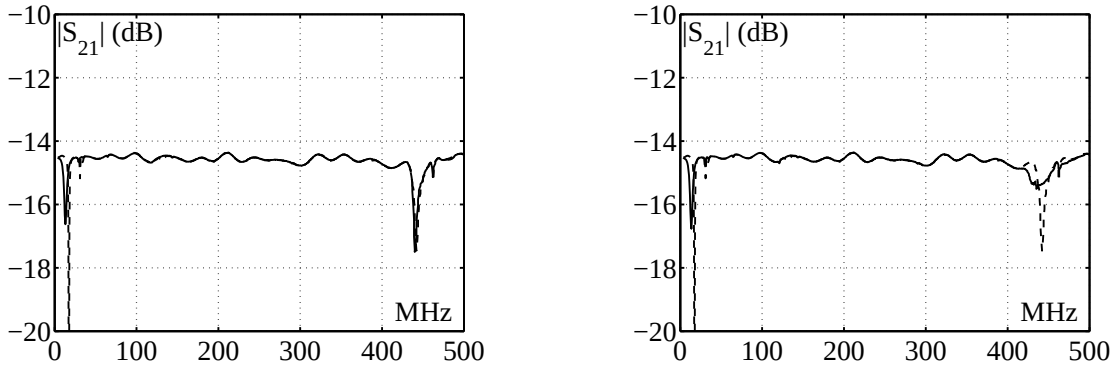

Figure 10: Transmission coefficient between the ends of the ceramic chamber. The dotted lines are measured in normal conditions while the solid line are measured where a lossy ferrite (Emerson-Cuming Type ZN) is placed around the position "**A**" (left picture) and "**C**" (right picture) defined in Fig. 5.

3.7 Field leakage

As a direct proof for external image currents magnetic field probes were used (Type HP11940 for the 30 MHz-1 GHz range and Type HP11941 for the 9 kHz-30 MHz range) and the relative field intensity near the ceramic pipe was measured as a function of frequency. Note that these are relative and uncalibrated data, i.e the sensitivity of the field probes (increasing with frequency) is not taken into account(Fig 11). One can clearly recognise that the maxima of the leakage field coincide with the resonances found by the wire method (Fig. 11, left plot) and the standing wave pattern related to the length of the ceramic pipe (Fig. 11, right plot).

4 Conclusion

It has been shown experimentally using the coaxial wire method that the image current is changing its azimuthal distribution drastically over the low frequency range. For very low frequencies, where the shielding strips are not yet contributing, nearly all the image current is passing over the "cold conductor" (bypass effect). The validity of this statement for beam induced image currents will be checked later in a separate paper with a numerical/analytical approach. Then we have identified a kind of transition region,

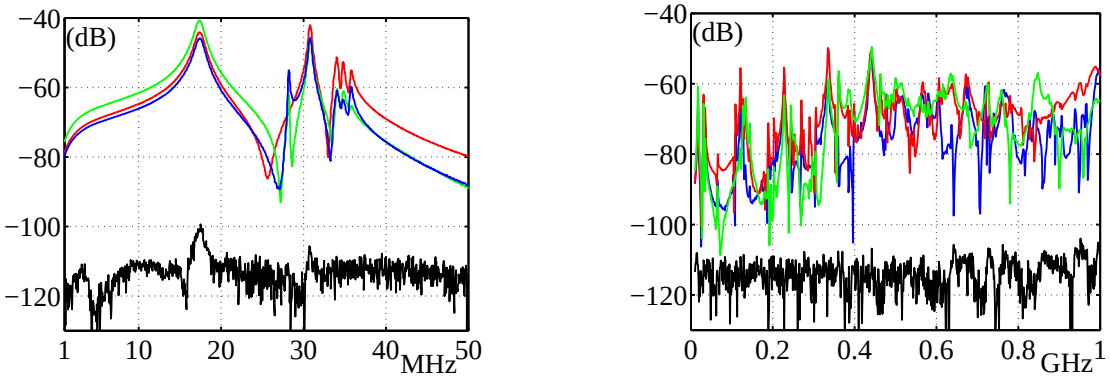

Figure 11: Field outside the ceramic chamber. One port of the VNA is connected to the wire inside the chamber and the other port to a field probe. In the pictures, the transmission coefficient between the wire and the probe is plotted for different positions of the probe along the chamber. The probe has been placed at the positions marked "**A**" (violet curves), "**B**" (blue curves), "**C**" (red plots) in Fig. 5. The wire is coaxial line is terminated on 50 Ω. The black lines are measured with a probe far away from the chamber. (IF=30 Hz, power 10 dBm).

where the image current partly passes via the "cold conductor" and partly via the shielding strips. In this transition region also strong resonances show up from the LC circuit formed by the printed coupling capacitor and the inductance of the loop formed by the shielding strips and the cold conductor. We must keep in mind in this transition region surface currents both on the inner and outer surface of the strips are present and that the thickness of the strips is in the order of a skin depth, leading to a rather complicated electromagnetic boundary value problem. Having done several experiments it was found that one or more ferrite rings of suitable material (losses!) can effectively dampen the resonances mentioned above as well as another small resonance around 500 MHz, which is related to the length of the (printed) coupling capacitor. A detailed evaluation of this option will be done later when a real prototype of the inner ceramic chamber is available and also proper RF contacts to the end plates of the vacuum tank can be provided. From the results obtained on the 1 meter long test chamber it can be stated that above this transition region (10-30 MHz) the concept of capacitively coupled shielding strips works well and leads to very small longitudinal coupling impedances (in the order of a few Ohm) which are mandatory for the LHC operation.

5 Acknowledgements

We are grateful to R. Garoby and F. Ruggiero for support, L. Ducimetiere as well as N. Garrel, J. Bertin and J.C. Guillot for patient and persistent help and L. Vos and D. Brandt for discussions.

References

[1] F. Caspers, A. Mostacci and B. Spataro, *On trapped modes in the LHC recombination chambers: experimental results*, LHC Project Note 266, CERN, August 2001; see also LHC Project report 604, CERN, August 2002.

[2] F. Caspers, C. Gonzalez, H. Tsutsui, M. Dyachkov, *Impedance Measurements on the LHC Injection Kicker Prototype*, LHC Project Note 219, CERN, March 2000.

[3] F. Caspers, *Impedance Determination from Bench Measurements*, Handbook of accelerator physics and engineering, A.W. Chao and M. Tigner (editors), World Scientific, Singapore, 1999.
[4] *Response Error-Correction for Transmission Measurements*, HP 8753D Option 011 Network Analyser: User Guide, p. 5-10.